IASS 2024 Symposium
Redefining the Art of Structural Design
August 26-30, 2024, Zurich Switzerland
Philippe Block, Giulia Boller, Catherine DeWolf,
Jacqueline Pauli, Walter Kaufmann (eds.)

Modular Lattice Bridges Inspired by Système Eiffel

Henrique M. MARTINS*, Ashley P. THRALL[a]

*, [a] Kinetic Structures Laboratory, Department of Civil & Environmental Engineering & Earth Sciences,
University of Note Dame
156 Fitzpatrick Hall, Notre Dame, IN 46556 USA
hmarti22@nd.edu

Abstract

This paper presents the development and numerical investigation of a novel form for resilient lattice bridges inspired by the Système Eiffel. While Gustave Eiffel is known for his major works of structural art (e.g., Maria Pia Bridge), he was also a pioneer in modular and rapidly erectable bridges that were used worldwide. His Système Eiffel consists of triangular modules, with each module being made up of angle sections. These are joined to one another in an alternating fashion, with adjacent modules rotated 180 degrees. The same module could achieve a variety of spans (6-21 m), and deeper versions were used for longer spans (up to 30.8 m). Inspired by Eiffel, but factoring in today's economic and labor market, this research has developed a novel approach to modular lattice bridges. Specifically, this research harnesses Eiffel's approach of rotating adjacent modules, but instead focuses on the connector as the module that joins standard sections. Importantly, the lattice-type layout provides the structure with system redundancy, meaning that the fracture of one member does not cause collapse. This paper presents the numerical investigation of these modular lattice bridges through finite element analyses, considering behavior under dead and live load, global stability, and performance when subjected to member loss.

Keywords: Lattice, bridge, modular design, rapid construction, redundancy, resiliency

1. Introduction

Bridge design typically uses a one-of-a-kind approach for each location. While this approach can offer flexibility, it often comes at the expense of increased construction time and cost. It is not uncommon for unique solutions to require custom analysis and detailing, occasionally involving complex configurations, which can also hinder fabrication and field assembly. In contrast, modular technologies hold great potential to streamline and maximize efficiency in the bridge industry. As identical modules can be used repeatedly within one structure and/or among many structures, one set of shop drawings can be created and modules can be mass-produced, leading to major savings in cost and time.

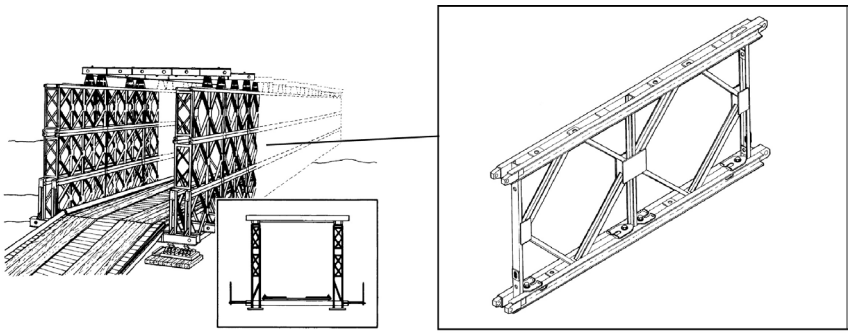

Figure 1: Bailey Bridge. Images from Department of the Army [1], with minor adaptations.

The state-of-the-practice in modular bridge technologies includes panelized systems, where panels are connected longitudinally by pins and are stacked transversely and/or vertically to achieve longer spans or higher load carrying capacities. These arose from the Bailey Bridge (Figure 1), developed in response to bridging needs from World War I and World War II (Joiner [2], Russell and Thrall [3]). More recently, research has evaluated different configurations for panels (Gerbo et al. [4]), developed alternative modules (Wang et al. [5]), and used topology optimization to investigate new panel designs (Tugilimana et al [6], [7], [8], [9]).

As reviewed in Thrall [10], before the development of these modern panelized systems, however, Gustave Eiffel developed a lightweight, modular system composed of steel triangular modules which could be assembled with limited equipment and labor (Eiffel [11], [12], [13]), popularized as the Système Eiffel (Figure 2). Each triangular modular is comprised of angle sections joined by gusset plates and bolts. These are combined in an alternating fashion, with adjacent modules rotated 180 degrees to one another (blue versus red). Using this module, the Système Eiffel could achieve spans from 6 - 21 m, with deeper versions also available to reach spans up to 30.8 m (Eiffel [11], [12], [13]). While Eiffel is well known for his contributions to the design of major arch bridges [e.g., Maria Pia Bridge (Thrall et al. [14], Thrall [15])], his Système Eiffel was used widely across the world.

Inspired by the alternating modules of the Système Eiffel while also incorporating modern fabrication technologies and prioritizing redundancy, this paper introduces a new system: a modular lattice bridge (Figure 3). This paper numerically investigates the behavior of this system under service loads and when subjected to the loss of a tensile member.

2. Modular lattice bridges

The novel modular lattice bridge (Figure 3) aims to combine the cost and time benefits of modularity with the multiple load paths available through a lattice-type topology.

Inspired by the alternating orientation of the Système Eiffel, the members - which in this case are WT sections - alternate in directionality (blue versus red). They are connected by “lattice joints” [Figure 3 (a and b)], made up of flat flanges welded to flat web plates. Here, the lattice joints, which can be mass-produced in a shop environment, are the module. The WT members are standard and readily available. The WT members and the lattice joints would be connected via bolted splice connections (not shown) for rapid erection in the field (i.e., no field welding). The alternating diagonal components (blue versus red) are not connected to one another. The upper and lower chords are comprised of back-to-back WTs that are bolted to one another [Figure 3 (f and g)] and to their corresponding lattice joints. Overall, this follows the concept of modularizing the connector and using standard sections as members introduced in Tumbeva et al. [16], [17], [18] and Tumbeva and Thrall [19]. This framework, as opposed to the triangular modules introduced by Eiffel, works within modern fabrication and erection approaches.

This system also aims to take advantage of module stacking consistent with modern panelized bridges. Figure 3 (c, d, and e) shows the same system in a single, double, or triple stacked configuration, respectively, for increasing structural depth. It uses wide flange section floor beams and a lightweight deck that spans between the floor beams, similar to that used in modern panelized bridges. Importantly, it overcomes a disadvantage of these panelized bridges: that the panel stacking can lead to high concentrations of material at the neutral axis. Instead, this system concentrates material at the upper and lower chords with the back-to-back WTs.

Furthermore, the lattice topology provides multiple load paths. As this paper will numerically demonstrate, the modular lattice bridges are system redundant, meaning that the fracture of one member does not cause collapse of the entire bridge (AASHTO [20]). This offers enhanced safety and resiliency.

This paper focuses on the double-stack arrangement [Figure 3 (b)], with 30.5 m (100 ft) span length, 3.05 m (10 ft) depth, and 4.27 m (14 ft) width for one vehicular lane of traffic. Each module has a 3.05 m (10 ft) length and a 1.52 m (5 ft) depth between lattice joints (Figure 4).

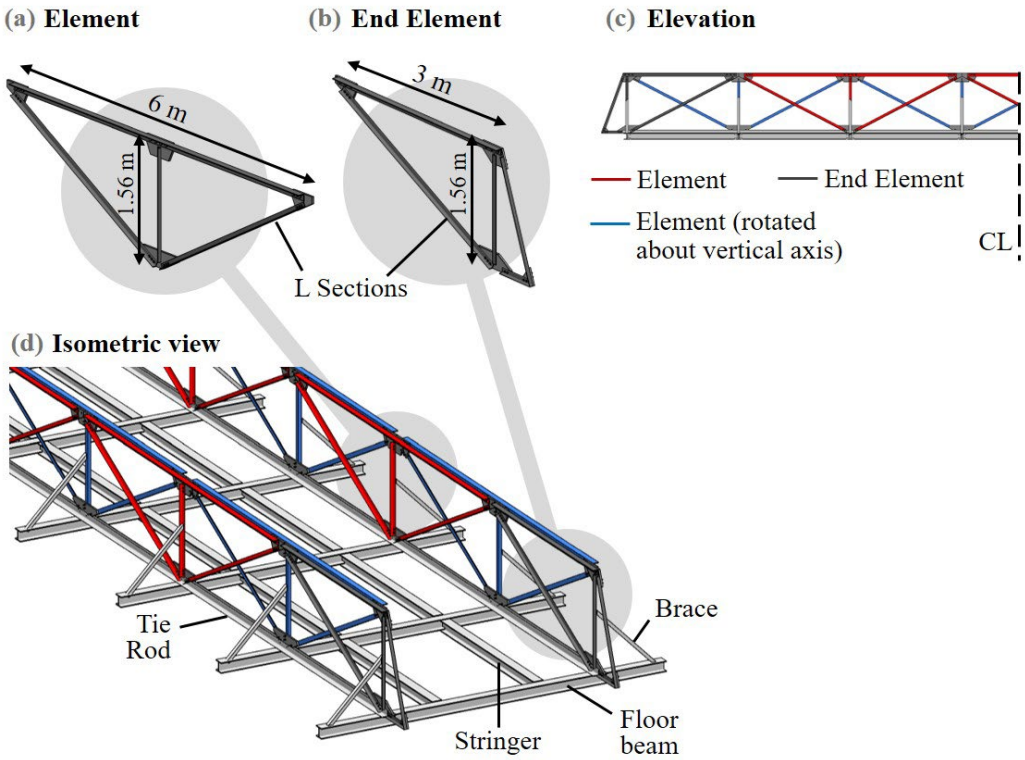

Figure 2: Système Eiffel

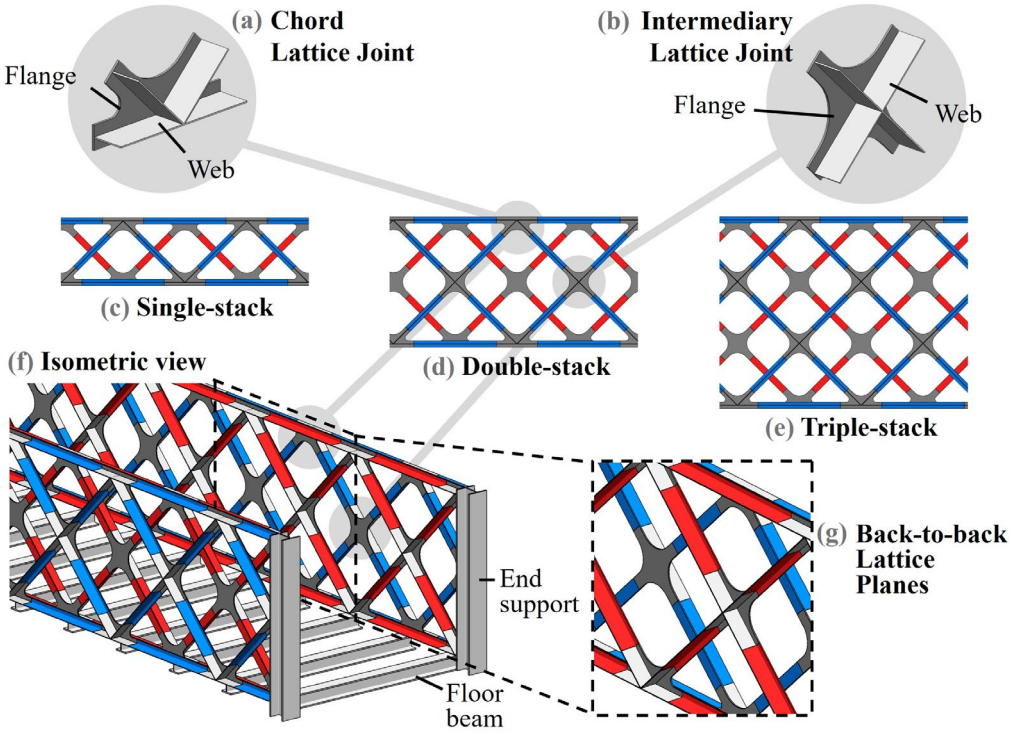

Figure 3: Modular lattice bridges.

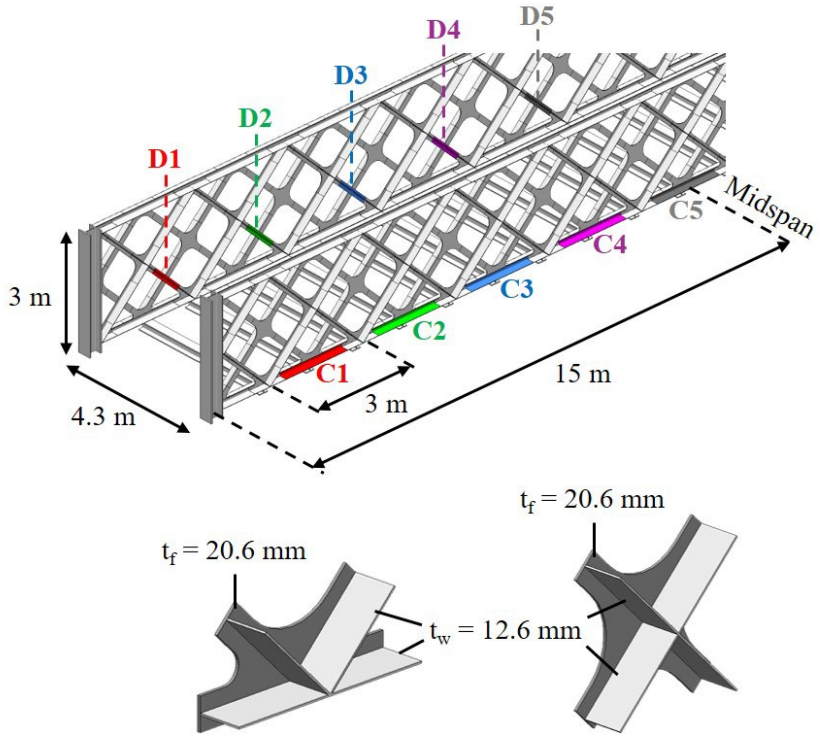

Figure 4: Double-stack geometry and section sizes.

3. Finite Element Numerical Models

This modular approach to resilient lattice bridges is evaluated under dead and live loads through three-dimensional (3D) finite element (FE) numerical models in the software package ABAQUS (ABAQUS [21]) [Figure 5]. Static and linear eigenvalue buckling analyses were performed, using the modeling assumptions, loads, and load combinations discussed in this section.

3.1. Model Assumptions

All components were modeled using four- or three-node reduced integration shell elements (i.e., S4R or S3R element types, respectively). A mesh size of 25.4 mm (1 in.) was used for all components.

Linear geometry was assumed.

A nonlinear material model with linear strain hardening was used, assuming a yield strength of 345 MPa (50 ksi), a modulus of elasticity of 200 GPa (29000 ksi), and an ultimate strength of 450 MPa (65 ksi) at a strain of 0.0476, based on the recommendations of AASHTO [20].

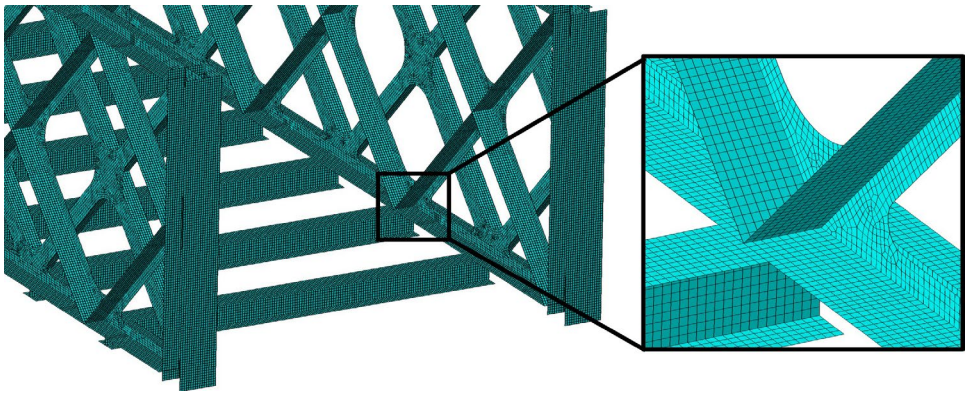

Figure 5: Finite element numerical model.

Boundary conditions on one abutment of the bridge included: vertical and longitudinal translation restrained. On the other abutment, only vertical translation is restrained. On one plane of the bridge, transverse translation is restrained for stability. These boundary conditions are applied to a single node at the center of gravity of the wide flange end components [Figure 3 (f)]. All flange and web nodes at the bottom surface of the wide flange node are then constrained to this node.

3.2. Applied Loads

Behavior is evaluated under dead load (DL) and live load (LL).

Dead load included the weight of the steel components. A superimposed dead load of a lightweight grid deck [0.718 kN/m² (15 psf)] was also considered.

Live load included one lane of vehicular traffic, according to the HL-93 design vehicular load prescribed by current American bridge design code (AASHTO [22]). This included a uniform lane load of 9.3 kN/m (0.64 klf) and a truck load comprised of 3-point loads (three axles) with 4.27 m (14 ft) center-to-center spacing and magnitudes of 35.6 kN (8 kips), 142 kN (32 kips) and 142 kN (32 kips). Note that a tandem [two 111 kN (25 kips) loads spaced at 1.22 m (4 ft)] would also need to be evaluated for design, but was excluded for simplicity in this paper. A multiple presence factor of 1.2 was applied as there is only one lane of vehicular traffic.

3.3. Load Combinations

Behavior of the system was evaluated under Service II load combination as prescribed by American bridge design code, which is:

$$\text{Service II: } 1.0\ \text{DL} + 1.30\ (\text{LL} + \text{IM}) \tag{1}$$

for the simplified loads considered in this study. The dynamic load allowance, IM, was taken to be 33% and was only applied to the design truck (AASHTO [22]).

To evaluate system redundancy, two redundancy load cases were also considered, as prescribed by the *Guide Specifications for Analysis and Identification of Fractural Critical Members and System Redundant Members* (AASHTO [20]). First, Redundancy I load case was evaluated to investigate the immediate effect of member fracture. This load case, simplified for the loads in this study, is:

$$\text{Redundancy I: } (1 + \text{DA}_\text{R})[1.05\ \text{DL} + 0.85\text{LL}] \tag{2}$$

Here, the dynamic impact of member loss is captured in a static analysis through the dynamic amplification factor, DA_R (for this structure, DA_R=0.4). The procedure followed for Redundancy I was: (1) apply factored dead load, (2) apply factored live load, (3) induce fracture, and (4) amplify loads. The long-term behavior of the faulted structure (e.g., in the case that a fracture is not detected and the bridge remains in use) was analyzed using Redundancy II load case. This load case, again simplified for the loads in this study, was:

$$\text{Redundancy II: } 1.05\ \text{DL} + 1.30(\text{LL} + \text{IM}) \tag{3}$$

For this load case, the dynamic load allowance, IM is 15% (AASHTO [20]). The procedure followed for Redundancy II was: (1) apply factored dead load, (2) induce fracture, and (3) apply factored live load. The methodology for evaluation of system redundancy, which follows the approaches prescribed in AASHTO [20] will be discussed further in a subsequent section.

4. Behavior

4.1. Behavior under service loads

The section sizes for the members (WT 9x35.5), the thicknesses for the lattice joints [20.6 mm (13/16 in) flanges and 12.6 mm (1/2 in) webs], the section size of the end supports (W 14x159) and the section size of the floor beams (W 10x88) were designed for the following performance metrics under the Service II load combination: (1) peak stress in any component is less than 55% of the yield stress, as

evaluated through a static analysis and (2) smallest positive eigenvalue greater than 1.5, as evaluated through a linear eigenvalue analysis. The former performance metric is chosen as a reasonable efficiency for material use. The latter performance metric focuses on the global stability of the system.

The results from analysis under Service II (Figure 6) indicate a maximum stress of 140 MPa (20.3 ksi) at the top chord, particularly where the connection between the two planes is made. This value represents 40.6% of the yield stress, being in the low to moderate range and, therefore, considered conservative. Stresses at the diagonals are generally lower than 20 MPa (2.90 ksi) and no larger than 50 MPa (7.25 ksi). This indicates the possibility of making the diagonals lighter or reducing their number closer to midspan, where shear stresses are lower and less material is needed close to the neutral axis, increasing efficiency.

Results from the buckling analysis (Figure 7) show a local buckling mode at the top chord, with a factor of 2.22, meaning that the structure can withstand all the applied loads multiplied by a factor of 2.22 before experiencing buckling. Additionally, the local mode suggests a less critical failure when compared to a global buckled mode shape.

Although lighter sections could be used, as mentioned above, such a decision could potentially change the buckled shape into a global shape, resulting in a less conservative design. Further, the focus was on having the diagonals and chords be the same section size to minimize the number of different sections used throughout.

The effects associated with thermal movement were investigated in accordance with AASHTO [22], but were found to be negligible.

4.2. Behavior when subjected to member loss

System redundancy was investigated through static analysis using the Redundancy I and Redundancy II load combinations. To simulate member loss, the member was "softened" by progressively reducing its modulus of elasticity as recommended in AASHTO [20]. Member loss was considered for tensile diagonals and tensile chord members identified as shown in Figure 4. The longitudinal position of the design truck was moved to coincide with the region of the fracture, in accordance with AASHTO [20].

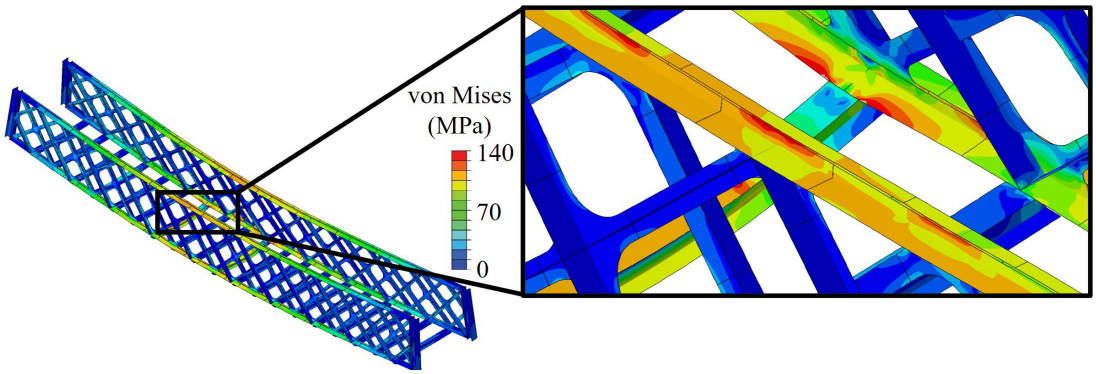

Figure 6: Stresses under service loads.

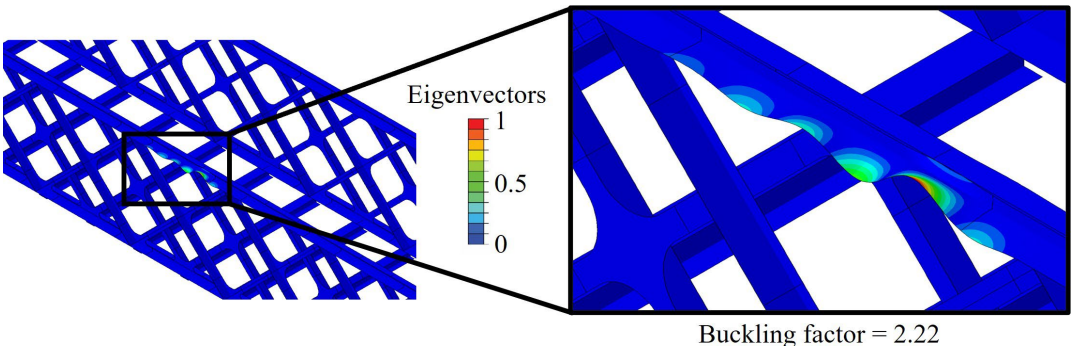

Figure 7: Buckled mode shape.

Specific local performance criteria for system redundancy include: (1) average strain in a primary member is less than five times the yield strain [0.00172 for 345 MPa (50 ksi) steel], (2) average strain in a primary member is less than 0.01, and (3) strain anywhere in a primary member is less than 0.05 (AASHTO [20]). Additionally, from a global perspective, the load-displacement performance was evaluated to ensure that the structure can continue to carry load up to an additional 15% of the factored live load (AASHTO [20]).

The most extreme scenario for chord loss would be loss of the bottom chord at midspan (C5). Considering Redundancy I (i.e., at the moment of member fracture) for the loss of chord C5, the peak strain in a primary member was found to be 0.00270 and the average strain in the same member was 0.000631. Both meet the aforementioned strain limits specified in AASHTO [20]. Figure 8 (a) shows the stress just prior to the fracture and Figure 8 (b) shows the stress just after. The peak von Mises stress prior to fracture [120 MPa (17.4 ksi)] increases at the regions where the fractured chord was connected to the lattice joints by 188% to 345 MPa (50.1 ksi). This suggests that the members analyzed reached yield, but not ultimate strength. A load transfer mechanism can be observed from the previously connected lattice joints to the remaining chord member at midspan.

Comparing the service behavior of the undamaged bridge [Service II; Figure 9 (a)] and the long-term behavior of the faulted structure when chord C5 is lost [Figure 9 (b)], there is negligible difference in the global stress distribution, as the structure is highly redundant and capable of redistributing the stresses along the span uniformly.

Considering the extreme case for diagonal loss (i.e., the loss of the diagonal D1 near the support under Redundancy I), the peak strain in a primary member was 0.00100 (at the lattice joint next to the fractured diagonal), while the average strain in the same member was 0.000207, both below the limits specified in AASHTO [20]. There were no considerable changes to the stress distribution from the fracture (Figure 10). Peak stresses at the diagonals reached approximately 27.4 MPa (3.97 ksi) before fracture [Figure 10 (a)], compared to 90 MPa (13 ksi) after fracture [Figure 10 (b)]. Although an increase of 63.6% was observed, those values are not concerning, as they represent a small percentage (16%) of the yield stress.

Considering the long-term behavior of the faulted structure (i.e., Redundancy II), load-displacement curves for each diagonal and chord loss scenario were developed (Figure 11). For these analyses, the design truck was placed at midspan (as opposed to at the location of the fracture) to better compare performance. As can be observed visually, there was very little loss of stiffness due to any of the fractures, as compared to an undamaged bridge, even when incorporating an additional 15% of the live load. Loss of Chord C5 [Figure 11 (a)] resulted in a stiffness of 44.8 kN/mm or 92.5% of the undamaged stiffness (48.4 kN/mm). The worst case of diagonal fracture [loss of Diagonal D5 in Figure 11 (b)] showed a stiffness of 47.0 kN/mm or 97.1% of the undamaged stiffness. This further demonstrates the capability of the modular lattice system to redistribute load effectively.

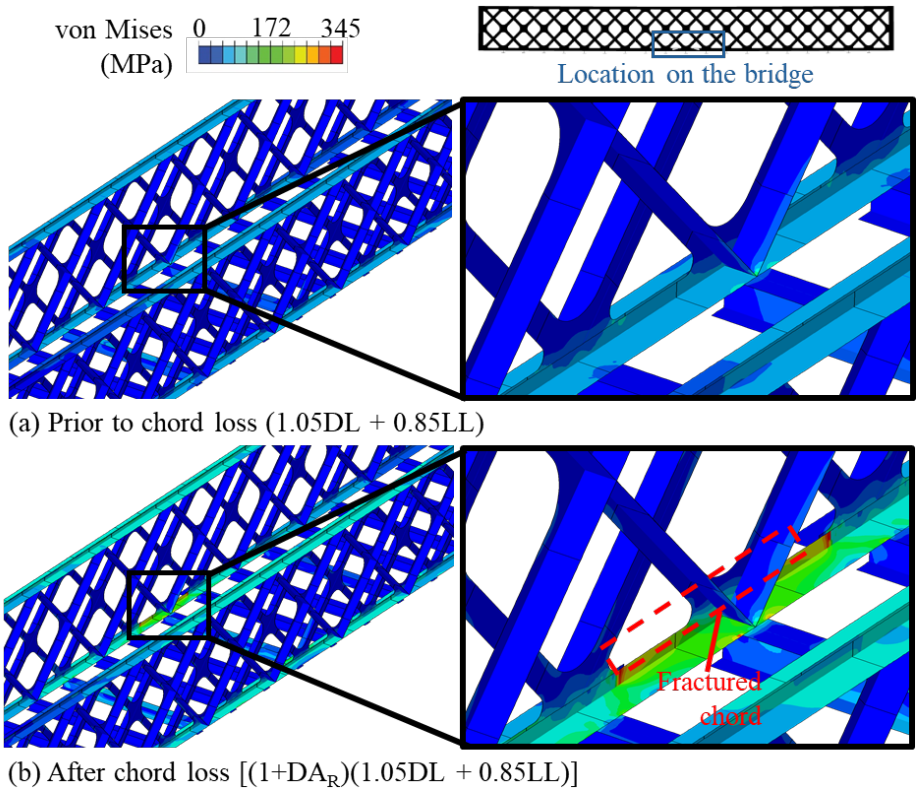

Figure 8: Stresses variations due to immediate effect of fracture of Chord C5: (a) prior to chord loss and (b) after chord loss (Redundancy I).

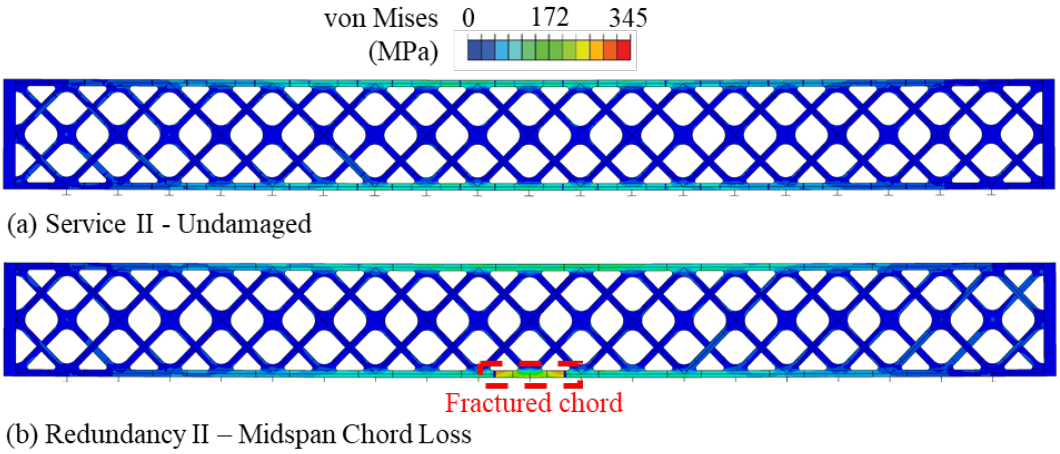

Figure 9: Stress variations considering long-term behavior: (a) undamaged bridge (Service II) and (b) considering loss of Chord C5 (Redundancy II).

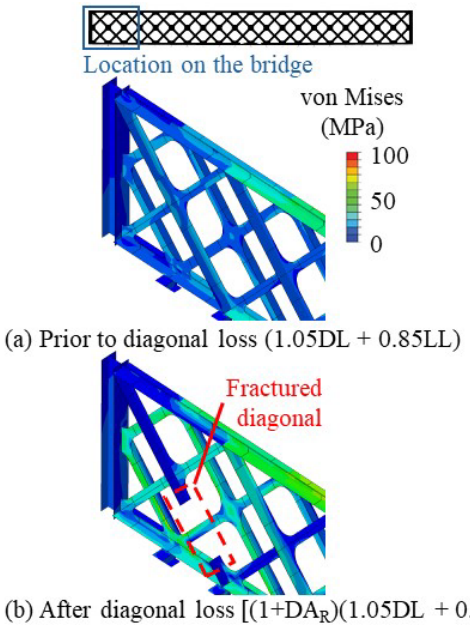

Figure 10: Stresses variations due to immediate effect of fracture of Diagonal D1: (a) prior to diagonal loss and (b) after diagonal loss (Redundancy I).

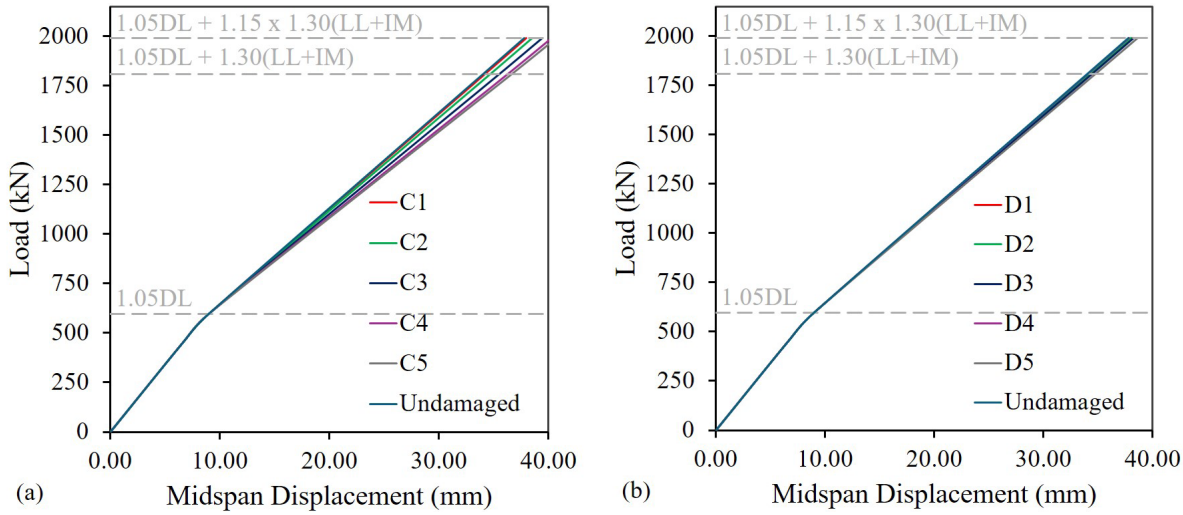

Figure 11: Redundancy II: Load-displacement behavior considering (a) chord loss and (b) diagonal loss.

5. Conclusion

This paper presented a novel approach for modular lattice bridges inspired by the Système Eiffel. It harnesses the benefits of lattice-type structures (i.e., capability to redistribute load through multiple paths) and cost-effectiveness of modular construction. To incorporate today's labor and economic market, this approach focused on "modularizing" the connection and using standard section sizes that are readily available. Detailed 3D FE analyses were performed to numerically demonstrate performance under service loads as well as system redundancy.

This paper specifically focused on the performance of a 30.5-m (100-ft) long, single lane vehicular bridge which represents a "double stack" configuration. Future work will also evaluate single and triple stack configurations, as shown in Figure 3, toward a comprehensive kit-of-parts system. Research will also focus on further development of the connector for optimized material use and incorporate fabrication considerations. Additional dynamic analysis can provide further insight into structural behavior.

Acknowledgements

This material is based upon work supported by the National Science Foundation under Grant No. TI-2044340.

References

[1] Department of the Army, "Bailey bridge," *Field Manual No. 5-277*, Headquarters, Dept. of the Army, Washington, DC, 1986.

[2] Joiner, J. H., *One More River to Cross: The story of British Military Bridging*, South Yorkshire, UK: Pen and Sword Books, 2001.

[3] Russell, B. R., Thrall, A. P., "Portable and Rapidly Deployable Bridges: Historical Perspective and Recent Technology Developments," *Journal of Bridge Engineering*, 18(10), 1074-1085, 2012.

[4] Gerbo, E. J., Casias, C. M., Thrall, A. P., Zoli, T. P., "New bridge forms composed of modular bridge panels", *Journal of Bridge Engineering,* 21(4), 04015084, 2015.

[5] Wang, Y., Thrall, A. P., Zoli, T. P., "Adjustable module for variable depth steel arch bridges", *Journal of Constructional Steel Research*, 126, 163-173, 2016.

[6] Tugilimana, A., Filomeno Coelho, R., Thrall, A. P., "An integrated design methodology for modular trusses including dynamic grouping, module spatial orientation, and topology optimization", *Struct. Multidiscip. Optim.*, 60(2), 613-638, 2019.

[7] Tugilimana, A., Filomeno Coelho, R., Thrall, A. P., "Including global stability in truss layout optimization for the conceptual design of large-scale applications", *Struct. Multidiscip. Optim.*, 57(3), 1213–1232, 2018.

[8] Tugilimana, A., Thrall, A. P., Filomeno Coelho, R., "Conceptual design of modular bridges including layout optimization and component reusability", *Journal of Bridge Engineering*, 22(11), 04017094, 2017.

[9] Tugilimana, A., Thrall, A. P., Descamps, B., and Filomeno Coelho, R., "Spatial orientation and topology optimization of modular trusses", *Struct. Multidiscip. Optim.*, 55(2), 459-476, 2017.

[10] Thrall, A. P., "Celebrating Early Innovation in Modular Bridge Design: Système Eiffel," *Technology and Innovation*, In press, 2024.

[11] Eiffel, G., "Ponts Portatifs Économiques, Ponts Démontables," *Levallois-Perret: Compagnie des Établissements Eiffel*, 1890.

[12] Eiffel, G., "Constructions Métalliques et Entreprises de Travaux Publics," *Librairie des Dictionnaires, Paris*, 353-354, 1886.

[13] Eiffel, G., "Notice sur les Ponts Portatifs Économiques: Système Eiffel," *Paris: Imprimerie Paul Dupont*, 1885.

[14] Thrall, A. P., Billington D. P., Bréa K. L., "The Maria Pia Bridge: A Major Work of Structural Art," *Engineering Structures*. 40, 479-486, 2012.

[15] Thrall, A. P., "A Comparison of the work of Gustave Eiffel and Othmar Ammann: The Maria Pia and Bayonne Bridges lessons for 21st century design", Princeton (NJ), Princeton University, 2008.

[16] Tumbeva, M. D., Thrall, A. P., Zoli, T. P., "Modular joint for the accelerated fabrication and erection of steel bridges," *Journal of Bridge Engineering*, 26(6), 04021022, 2021.

[17] Tumbeva, M. D., Thrall, A. P., Zoli, T. P., "Investigating the redundancy of steel truss bridges composed of modular joints," *Journal of Constructional Steel Research*, 188, 107038, 2022.

[18] Tumbeva, M. D., Thrall, A. P., Zoli, T. P., "Modular joint for free-form undulating structures", In Proceedings of IASS Annual Symposia (Vol. 2018, No. 13, pp. 1-4), International Association for Shell and Spatial Structures (IASS), 2018.

[19] Tumbeva, M. D., Thrall, A. P., "Modular connector for resilient grid-shell structures," Journal of Structural Engineering, 147(8), 04021115, 2021.

[20] American Association of State Highway and Transportation Officials (AASHTO), *Guide Specifications for Analysis and Identification of Fracture Critical Members and System Redundant Members*, Interim Revisions AASHTO, 2022.

[21] ABAQUS, *ABAQUS/Standard Analysis User's Manual*. Waltham, MA, Dassault Systemes, 2022.

[22] AASHTO, *AASHTO LRFD Bridge Design Specifications*, 9th Edition, AASHTO, 2020.